Радиофизика и радиоастрономия, 2002, т. 7, №2, с. 121-138

# Millimeter-Wave Radars for Environmental Studies

D. M. Vavriv, V. A. Volkov, V. N. Bormotov, V. V. Vynogradov, R. V. Kozhyn, B. V. Trush, A. A. Belikov, and V. Ye. Semenyuta

*Institute of Radio Astronomy of the National Academy of Sciences of Ukraine*
*4, Chervonopraporna St., 61002, Kharkov, Ukraine*
*E-mail: vavriv@rian.kharkov.ua*

*Received January 16, 2002*

A review is given of recent activities undertaken in the Institute of Radio Astronomy of the National Academy of Sciences of Ukraine for the development of millimeter-wave radars. The radars constructed include cloud radars and a side-looking airborne radar system. They are capable to perform real-time, high-resolution measurements in the frequency bands of 36 and 95 GHz. The set-up of these instruments, the novel technical solutions, and the signal processing technique introduced are discussed. The results obtained with such instruments during measurement campaigns are presented as well.

## 1. Introduction

During the last five years in the Institute of Radio Astronomy several R&D projects have been fulfilled aimed at the development of mm-wave radars for environmental studies. In particular, we have constructed 95 and 36 GHz cloud radars and a dual-frequency (95 and 36 GHz) airborne side-looking radar.

Millimeter-wave Doppler radars are considered now as the most actual instruments for permanent monitoring and investigations of clouds. An idea of using cloud radars at millimeter wavelengths is based on the fact that the power of radar returns from cloud particles scales as $\lambda^{-4}$ ($\lambda$ is the wavelength) almost up to the wavelength of 3 mm. Therefore, both a high radar sensitivity and resolution can be achieved by using the radar transmitters with a relatively low output power and the antenna systems with moderate dimensions, as compared to those at lower frequencies. The above advantages enable the development of compact and transportable cloud radar systems. Another advantage of the millimeter-waves is related with a negligible role of reflections caused by the clear air turbulence. Such reflections manifest themselves substantially in radar returns at larger wavelengths, leading to a serious problem of identification of signals produced purely by the cloud particles.

The millimeter-wave cloud radars are typically produced to operate at the frequencies of about 36 and 95 GHz, which correspond to the atmospheric low-loss windows. The 36 GHz frequency band is considered now as the most suitable band for the development of ground-based radars, whereas 95 GHz radars have obvious advantages for performing observations from aircraft. However, combined observations at both these frequencies are rather promising. They allow to find the cloud particle size and velocity distributions, the water content, and other cloud parameters.

Until the beginning of the 90th, millimeter-wave cloud radars were available only at several institutions around the world, and they were used as laboratory instruments for non-regular cloud observations [1-3]. During the last decade, there are growing activities related both with the development and applications of the millimeter-wave radar systems [4-7]. Such activities have been stimulated by several international programs aimed at investigating the global climate change. It is believed that by means of such cloud radars it would be possible to investigate and understand in details the macro- and microphysical properties of clouds and their impact

on the Earth radiation budget and the hydrological cycle.

Nowadays cloud radar systems with a high sensitivity are required to study even rather weak and thin cloud layers. Such systems should be capable for long-term, unattainable operation and real-time, high-resolution measurements of various atmospheric characteristics, like profiles of radar reflectivity, Doppler spectrum and its moments, and polarimetric quantities. Besides, the radars should include a reliable system of permanent calibration, a possibility of a remote control, and a possibility of an access to radar data through a network. The cloud radars developed and produced in our institute [8-10] satisfy these requirements to a great extent.

The side-looking airborne radar [11], which will be also described in this paper, is used for the investigation of the radar scattering properties of various surfaces at the frequencies of 36 and 95 GHz simultaneously. At the first stage of exploitation, the radar system has been used for the study of millimeter-wave backscatter characteristics of water surfaces in the presence of oil films. This study has been aimed at the development of efficient instruments and methods for oil-spill detection and quantification. There are two main reasons for the application of millimeter waves rather than microwaves when developing instruments for oil pollution monitoring. Firstly, so far accumulated experimental data [12, 13] and recent theoretical results [14] indicate that radar contrast of the films becomes larger with increasing the radar operating frequency. Secondly, millimeter wave systems offer the well-known weight and portability advantages, what make their installation on a light-weight aircraft easy.

The above radar systems are described in this paper which is organized in the following way. In Section 2, general approaches and solutions to the development of the transmitters and the data acquisition system used in the both types of radars, are described. In Section 3, the 36 Doppler cloud radar is described along with examples of measurement results. The 95 GHz Doppler cloud radar is presented in Section 4. Section 5 contains a description of the dual-frequency side-looking radar and an example of its application for oil-spill detection. Section 6 contains a brief summary of this paper.

## 2. Radar Design Solutions

### *2.1. Radar Ttransmitters*

Usually, the choice of reliable high-power tubes for 36 and 95 GHz radar transmitters presents the most serious problem when developing the mm-wave radars with a long-distance operation range. The problem lies in the necessity to have the transmitters which should provide both a high peak and average power in order to achieve a high radar sensitivity and spatial resolution simultaneously. The transmitters for 36 GHz radars are usually based on conventional magnetrons or travelling-wave tubes (TWT). The magnetron transmitters, however, often suffer from a low reliability of conventional magnetrons for this frequency band [7]. The application of TWTs makes it necessary to use a pulse compression technique, since such tubes have typically a low level of the peak power, but they can operate with a high value of the duty factor [7]. Until recently, transmitters for 95 GHz radars have been mainly built on the basis of the klystron with extended interaction [4, 6]. This klystron surpasses the other tubes suitable for such radars in the average power provided, the dimensions, and the weight.

We have used an alternative way of developing both the 36 and 95 GHz radar transmitters. Our transmitters are based on spatial-harmonic magnetrons with cold secondary-emission cathode [15-17], which are produced in our institute. Compared with the classical magnetrons, such magnetrons can operate effectively at these frequencies and even at higher ones. Besides, they are characterized by smaller dimensions and weight, higher peak and averaged output power, and larger lifetime while maintaining other well-known advantages of magnetron tubes.

Our studies have shown that using specially designed modulator enables the development of transmitters with a rather high quality of output pulses [18, 19]. We have found that among various possible schemes of modulators, the scheme with partial discharge of the storage capacitor and a hard tube as high voltage switch is most suit-

able for driving both the 36 and 95 GHz spatial-harmonic magnetrons with cold cathode. The typical transmitter block diagram is shown in Fig. 1. The transmitter usually includes the following main parts: a high-voltage power supply, filament power supplies for the magnetron and the modulator tube, a driver for this tube, and a controller. The low-voltage power supplies were built by using a resonant technique to provide high efficiency and to suppress interference. The high power supply utilizes a flyback converter with a current feedback along with a voltage multiplier. Such scheme allows one to obtain a voltage ripple as low as 2 V with an output voltage of 20 kV and an output power of 500 W. The output stage of the hard tube driver is based on the two-pole scheme and provides a voltage swing of 1500 V with the rise and fall times less than 15 ns. All power supplies in the modulator are synchronized at the frequencies which are a multiple of the pulse repetition frequency of the transmitter.

The operation of the transmitters is controlled by a microprocessor, which provides a smart mode of transmitter operation and a possibility of the transmitter diagnostics. In particular, pulse-to-pulse programmable control of the pulse repetition frequency is introduced. Local and remote control of the transmitters are made possible.

The above solutions enabled us to obtain the output transmitter pulses of a rather good shape and with a negligibly small jitter. The intrapulse phase change during the high power period of the 200 ns pulses is about 10° and 20°, and the pulse-to-pulse frequency chirp is reproducible to about 100 Hz and 300 Hz for the 36 and 95 GHz transmitters, respectively. The pulse jitter is less than 2 ns. The jitter occurs only at the initial stage of the pulse formation.

In order to illustrate the high quality of magnetron transmitters introduced in a 36 GHz radar system, a Doppler spectrum from a stationary ground based target at 12 km is shown in Fig. 2. A dwell time of 0.1 s and a pulse repetition frequency of 5 kHz were used in the measurements. It appeared that the width of the spectrum around zero frequency is 10 Hz at the level –5 dB and 20 Hz at the level – 45 dB, and it is determined by the dwell time rather than by the phase insta-

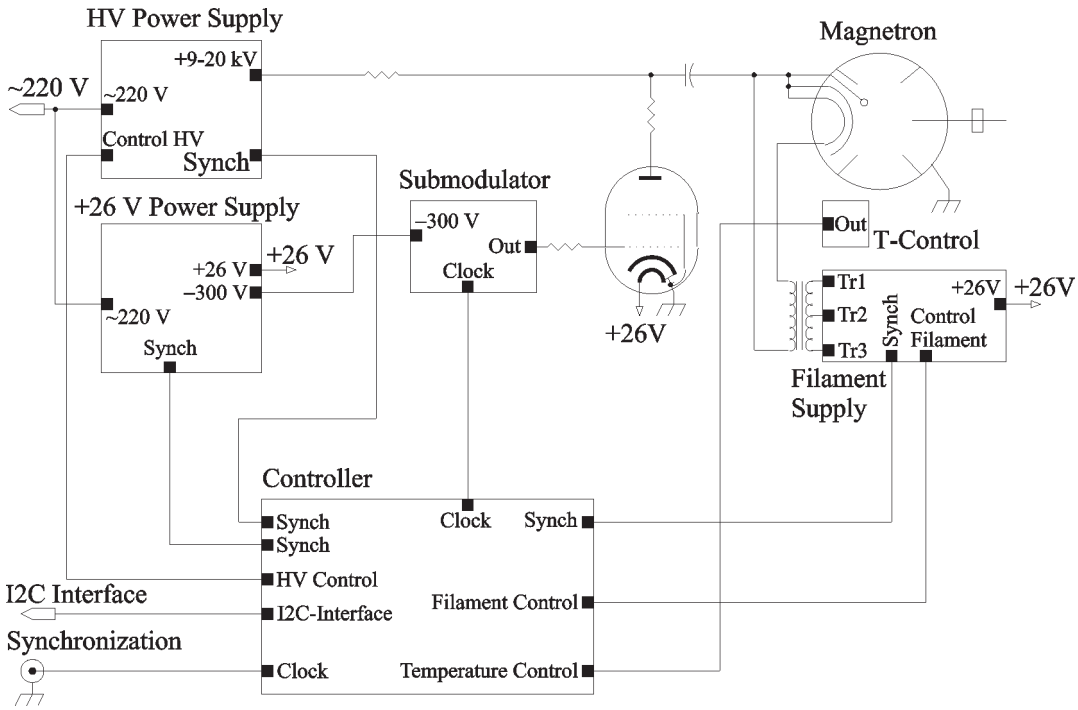


**Fig. 1.** *Typical block-diagram of the radar transmitters*

bilities of the transmitted pulses. It is also seen from this figure that the power density in the vicinity of zero frequency is about 50 dB higher compared to that in other spectral components.

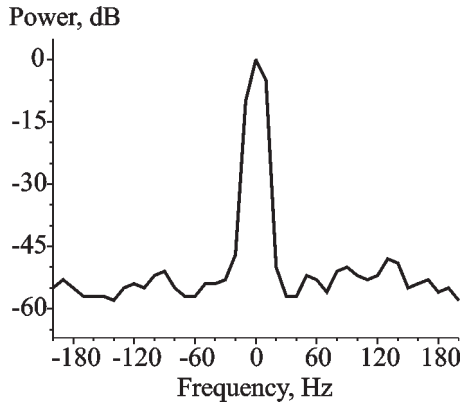


**Fig. 2.** *Doppler spectrum from a stationary ground based target at a distance 12 km obtained with a 36 GHz Doppler radar*

The achieved high quality of output pulses of the transmitters predetermined the application of a coherent on receiver technique for the realization of Doppler spectrum measurements.

### *2.2. Data Acquisition System*

Modern radars for environmental studies are multipurpose and complicated instruments. This calls for the development of corresponding hardware and software to provide real-time signal processing, representation, and storing of the radar data. Recent advances in programmable digital signal processors (DSP) together with novel approaches in signal processing and programming techniques allow the development of a cost-effective, universal data acquisition system with a wide range of application. We have developed such data acquisition system [20], which have been successfully implemented in both the side-looking dual frequency radar and the cloud radar systems.

The elaborated data acquisition system includes the following main components and corresponding software: (i) pre-processing board with a DSP, flash programming gate array (FPGA), and A/D converters; (ii) routines for DSP, providing input and performing preliminary processing of data; (iii) software package installed on a host computer performing interface between all the DSP on the ISA or PCI busses, reading preliminary processed and compressed data from the DSP, and performing other necessary functions (see below).

The main problem in the development of the pre-processing board lies in the necessity to receive, process, and compress a large input stream of data and service information in a real-time operation mode. For example, in the case of the dual-frequency side-looking radar, the input data stream is about 40 Mbytes per second under the pulse repetition frequency of 5 kHz. This problem is effectively solved with the help of a combination of hardware and software signal processing in the board as illustrated in Fig. 3. The board provides also interface with radar transmitters and receivers. So, there are two channels, each of them consisting of an input amplifier with a level shift circuit and ADCs. In order to provide a fast time-variant gain control of the receivers, a 40 MHz, 10-bit DAC is introduced. There is also a 5 kHz, 8-bit DAC for manual control of the gain of the receivers. The board contains also a buffer RAM, a serial port interface, control and synchronization circuits, together with DSP and ISA or PCI bus interface.

The receiver quadrature outputs come into the ADC input. The sampling rate is typically 50 MHz with the resolution of 12 bit. The digitized signals are written into one of the RAM buffers. The presence of two buffers allows to minimize time losses and to organize an optimal data processing. The generation of control and synchronization signals is performed in the RAM synchronization and control module based on the FPGA. There is a serial port, which allows to receive and transmit signals from/to up to 32 external sensors or sub-systems, like gyroscopic sensor, altimeter, etc. The interface of the pre-processing board with the host computer is arranged through standard ISA or PCI busses. Parallel synchronous operation of several such boards is possible in the host computer.

A software package has been developed for the host computer to perform the final stage of

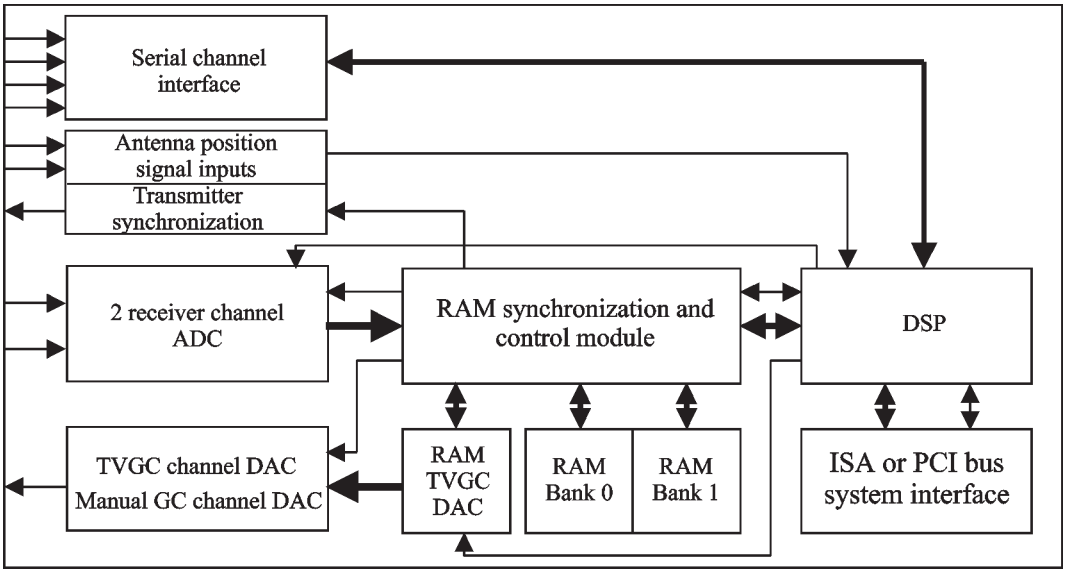


**Fig. 3.** *Combination of hardware and software signal processing in the board of the dual frequency radar*

the radar data processing. The package consists of the main program, which provides the user interface of the host computer and the interaction between other external devices; the library of additional functions performing the control of external devices (e. g., GPS receiver and aircraft orientation system connected to the computer through its serial ports); the virtual device driver performing the correct operation of the central processor and ISA or PCI cards in multitask operating system. In addition to the data processing and displaying, the package performs an independent control of the radar data channels (receiver TVGC, preliminary data processing, etc.). The controls are independent with respect to the real time data processing. This possibility can be realized only if the host processor operates under a multitask operating system. For this purpose we used OS Windows'98, NT, 2000, and Linux. A block diagram of the software package and its interaction with the hardware is presented in Fig. 4. Generally, the program represents a 32-bit multithread application. There are several reasons using the multithread approach. Firstly, the data from both pre-processing boards and serial ports of the host computer come asynchronously relative to the main program (i. e., by hardware interrupts). Then one can understand that a one-thread program cannot use the processor time optimally. Secondly, it is necessary to process radar data as well as to control both processing channels independently. In this case, the multithread approach together with thread synchronization tools, data buffering and object programming facilitate drastically the global architecture and debugging of the program. The data flows between the data processing software threads are shown in Fig. 4 by thick solid lines with arrows. The transfer roads of the control and the service information between the software modules are shown by solid lines and thick dashed lines with arrows, respectively. Thread 1a,b and Thread 3a,b have maximal time-critical priority. Thread 2 and Thread 4 are common for both radar data processing channels. Thread 4 is the main application thread. This thread provides the user interface, so it starts automatically after the program start. The user interface provides the option of a desired preliminary data processing routine. The user interface allows the operator to change preliminary data processing parameters (say, type of the TVGC function, slow or manual GC values, type and sizes of the averaging windows, etc.) without interrupting the real time signal processing. The operator can change the parameters determining the operation modes of Thread 3a,b performing the main data process-

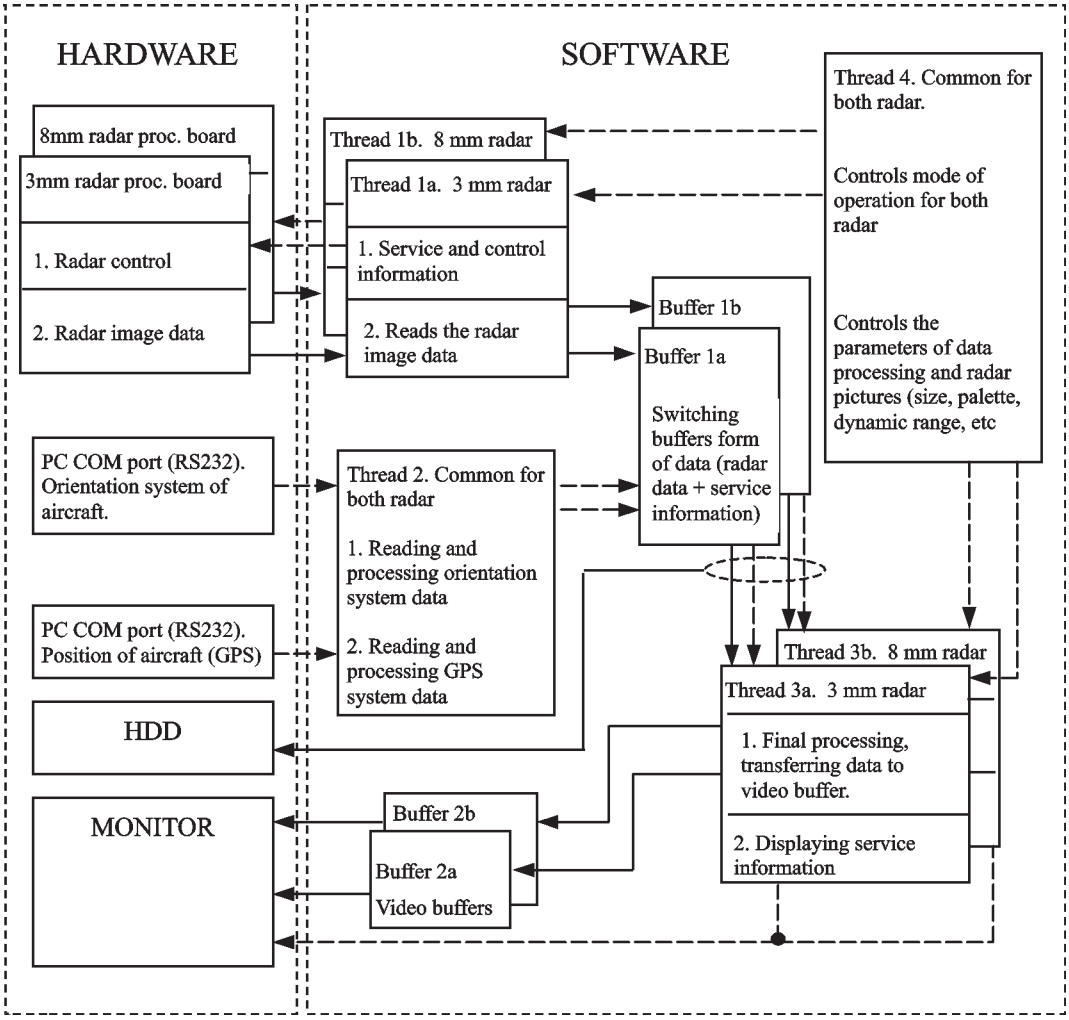


**Fig. 4.** *A block diagram of the software package and its interaction with the hardware of the dual frequency radar*

ing. For example, it is possible to change displaying parameters, namely the size, scale and the colour palette of radar image, the service information display parameters, the switch on and off data saving on HDD, etc. The software allows to browse and display radar data files saved before. A lot of additional service options for the data displaying analysis are available in the browsing/displaying regime.

## 3. 36 GHz Doppler Cloud Radar

### *3.1. Radar Characteristics*

The 36 GHz Doppler cloud radar to be described in this section was developed and produced in cooperation with Meteorologische Messtechnik GmbH, Elmshorn, Germany, during 2000. The radar was designed for unattended long-term operation to provide real-time permanent measurements of vertical profiles of the reflectivity, the mean velocity, the velocity variance, and the velocity spectrum. The possibility of raw data saving is also introduced. A permanent calibration system is included in the radar. The radar contains a server to provide remote control and data receiving.

Radar measurements are performed with the characteristics listed in Table 1. Corresponding characteristics of the 95 GHz Doppler radar, which will be described in Section IV, are also given in this table. The main technical parameters of the both radars are given in Table 2.

**Table 1.** *Radar measurement characteristics*

| | 36 GHz radar | 96 GHz |
|---|---|---|
| Minimum height, m | 200 | 200 |
| Measuring range, km | 15 | 15 |
| Range resolution, m | 15 – 60 | 7.5 – 60 |
| Doppler velocity resolution, m/s | 0.05 | 0. 1 |
| Maximum unambiguous velocity, m/s | ±15 | ±3.5 |
| Number of Gates (max) | 500 | 256 |
| FFT length | 128, 256, and 512 | 256 and 512 |
| Minimum dwell time, s | 0.1 | 0.1 |
| Antenna beam width, degree | 0.6 | 0.4 |
| Number of gates with simultaneous stored raw data | 8 | 2 |
| Sensitivity at 5 km with the integration time of 0.1 s, dBZ | –41 | –41 |

**Table 2.** *Technical parameters of the 36 GHz and 95 GHz cloud radars*

| | 36 GHz radar | 95 GHz radar |
|---|---|---|
| Peak power (max), kW | 30 | 4 |
| Pulse width, ns | 100 – 400 | 50 – 400 |
| Pulse repetition frequency, kHz | 2.5, 5, and 7.5 | 2.5 and 5 |
| Minimum detectable signal, dBm | –104 | –100 |
| Sampling rate, MHz | 50 | 20 |
| Sampling resolution, bit | 12 | 12 |
| Type of bus for the signal processing board | PCI | ISA |
| Operation system of the host computer | Linux or Windows | Windows |
| Network protocol | TCP/IP | |
| Antenna diameter, m | 1 | 0.5 |
| Antenna sidelobe level, dB | –20 | –20 |
| Power supply | 230V ± 10 % AC | 230V ± 10 % AC |
| Watt consumption (max), kW | 1300 | 700 |
| Weight, kg | 140 | 60 |

A block-diagram of the 36 GHz radar is shown in Fig. 5. The radar includes the following principal systems: an antenna system, a transmitter-receiver switch, two transmitters, one of which is used as a back-up transmitter, a receiver, a calibration system, a radar controller, a data acquisition and signal processing system, and a host computer. In addition, the radar has a waveguide ventilation system (not indicated in Fig. 5). The transmitter-receiver switch, the transmitters, the receiver, the calibration system, and the radar controller are placed in a transmitter-receiver rack (TRR), which is shown in Fig. 6 together with the radar antenna. During experi-

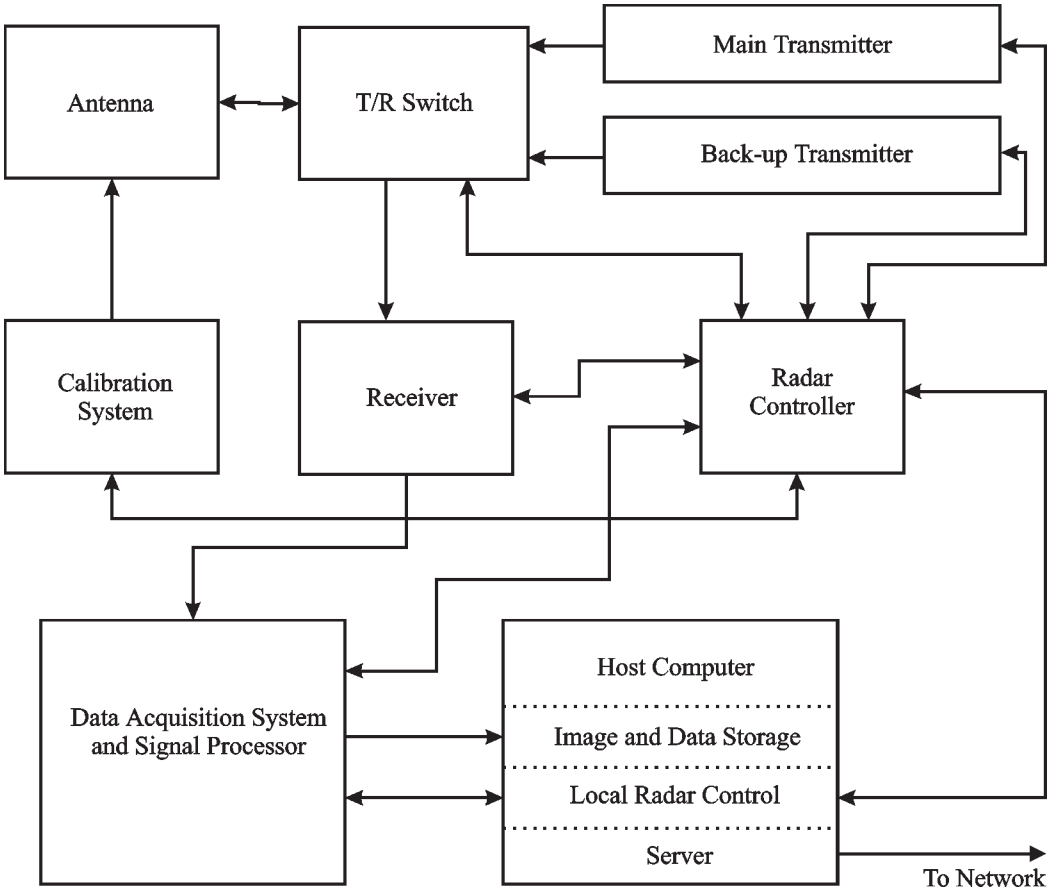


**Fig. 5.** *A block-diagram of the 36 GHz radar*

ments, the radar is typically placed in a car trailer. This allows to use it at remote locations at any weather conditions.

Recent advances in millimeter wave components, circuit design, and programming technique were implemented in the radar hardware and software. A Cassegrainian antenna with a 1-meter parabolic dish of 540 mm focal length is used. The antenna gain is 50 dB. The cross-polarization decoupling is better than – 40 dB. A corrugated horn with a $30°$ -mouth is used as the illuminator. The illuminator is protected from rain and dust by a Teflon™ cap. Holes are made in the antenna dish to evacuate water during rain. The antenna is lodged on a chassis, which enables pointing the antenna at any desirable angle.

The receiver was built by using only single frequency conversion to minimize the overall phase noise. The realization of such scheme became possible due to the introduction of a low noise synthesizer operating in the frequency band of 36 – 37 GHz and having the frequency step as low as 100 kHz. The receiver also benefits from the application of a mixer with a 3.5 dB noise figure and a 25 dB suppression of the local oscillator signal. A novel digital automatic frequency control loop is introduced to keep the difference between the magnetron and coherent oscillator frequencies less than 100 kHz with a high stability.

A digital coherence on receiver technique is realized. The phase of each transmitted pulse is stored directly in the digital signal processor and compared with the phase of reflected signal to calculate the Doppler velocity spectrum and its moments. The spectrum and the spectrum moments are measured simultaneously for 500 gates.

**Fig. 6.** *Transmitter-receiver rack together with the radar antenna*

The availability of a comprehensive control and diagnostic system is an important feature of this radar. The transmitters and receiver have their own controllers, which provide their programmable operation and a possibility of local and remote control and diagnostics. Totally, 29 radar parameters are controlled in real time, and the values of these parameters are stored in log-files, that simplifies essentially radar troubleshooting. Simultaneously, the controllers provide a safe radar operation by automatically controlling the radar parameters and switching off the radar in the case of dangerous situations.

The radar has a built-in permanent calibration system. The radar calibration is based on the independent measurements of the transmitter and receiver parameters. For these purposes, the transmitter output power and receiver sensitivity are continuously measured. The receiver sensitivity is determined by means of measurements of the signal to noise ratio of an additional signal with a constant power level. Such calibration system also enables evaluating the antenna surface conditions.

The radar has network capabilities allowing remote radar control and data receiving through any network supporting the TCP/IP protocol, including the Internet. In order to provide the network services, a special radar server is developed and introduced [21]. The server is working on the radar host computer under control of the Linux operating system. There is also a software package of Windows programs for obtaining and visualising radar data via the Internet. Remote control and diagnostics of the radar operation from any network computer is made possible as well.

The measured quantities, namely the reflectivity and velocity profiles, the velocity variance, and the Doppler spectrum are accessible in real time in various graphical and map forms on user displays of local and remote users. There are three levels of access to the radar. The first level, which is the level of the highest priority, includes a low level control and diagnostics of the whole radar system with a possibility to modify any radar parameters, including the internal parameters of the radar units. Such access is allowed only for qualified technical personnel. The second level of the radar control includes both local and remote high level control of radar operation, signal processing, data displaying, and data storing. Local and remote receiving of radar data and control of the mode of data displaying are made possible at the third level.

The user interface with the radar is organized as four display pages with corresponding menus. Each page forms a specific group of control elements: The first page, named DSP control, is used to control the DSP of the preprocessing card. The second page, named Radar control, is introduced to control the transmitter and receiver operation. The third page, named Processing control, is used to control the modes of row data processing, including data storage. The fourth page, named Image control, is for controlling the modes and parameters of the processed data viewing.

Example of configuration of the Image control page on the user display is shown in Fig. 7. The page includes a control panel and a data

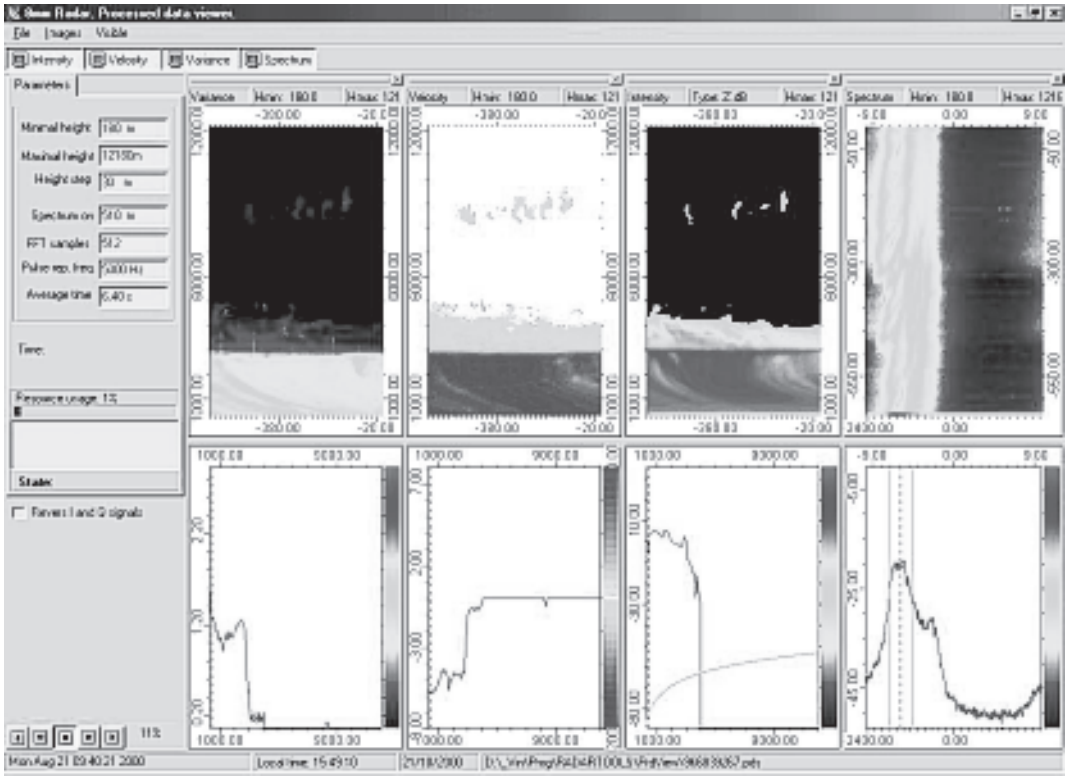

**Fig. 7.** *Example of configuration of the radar user display*

image panel. The control panel allows controlling radar operation in real time. On the data image panel, there are the intensity, velocity, variance, and the spectrum windows. Each of these four windows is divided into two subwindows. The upper part reflects the height-time map of the intensity, velocity, and variance in the case of the intensity, velocity, and variance windows, respectively. The lower part of these windows shows the instant oscilloscope plots of the incoming data. The instant oscilloscope plots can display either the horizontal or the vertical cut of the upper maps. For example, such cut may show the intensity versus time at some selected height (horizontal plot), or the intensity versus height (vertical plot). The upper plot of the spectrum window is the dynamical spectrum, where the vertical axis corresponds to the time and horizontal one to the Doppler frequency (or the corresponding velocity). The lower plot is an instant spectrum. Any of these windows may be temporarily hidden.

### *3.2. Examples of Measurements*

Typical examples of radar images of various types of clouds obtained with the 36 GHz cloud radar are presented in Fig. 8, 9, and 10. These figures show the vertical profiles of the reflectivity in terms of dBZ (left column) and the mean velocity (right column) in a time-height representation. The horizontal axes show the time in seconds, and the vertical ones show the height in meters.

In Fig. 8 cirrus clouds are shown. The base of such clouds is typically more than 6 km. In this case, the clouds occupy the layer from 6.5 km to about 11 km. From the velocity data, one can find the regions where the cloud particles are moving mainly in the up- and downward directions. However, the maximum velocities is less than 1 m/s. Notably higher particle velocities are seen inside the middle- and low-layer clouds shown in Fig. 9. These two types of clouds are clearly separated in space. The low-layer clouds are precipitating, but the precipitation does not

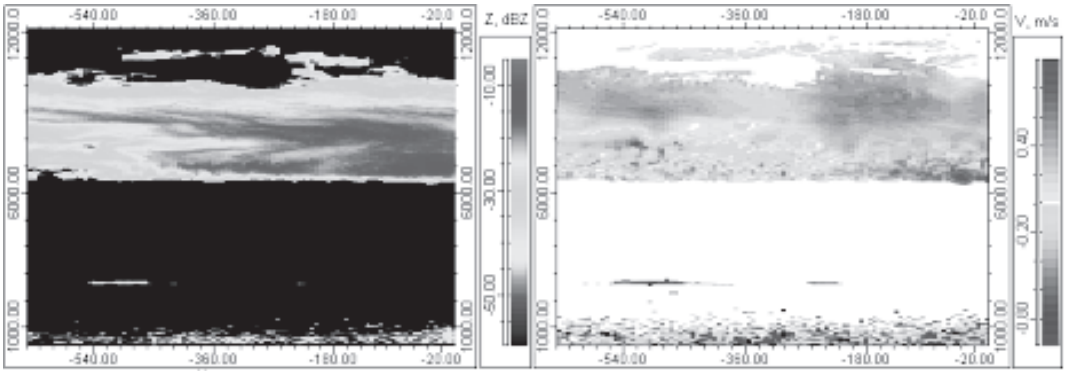


**Fig. 8.** *Cirrus clouds*

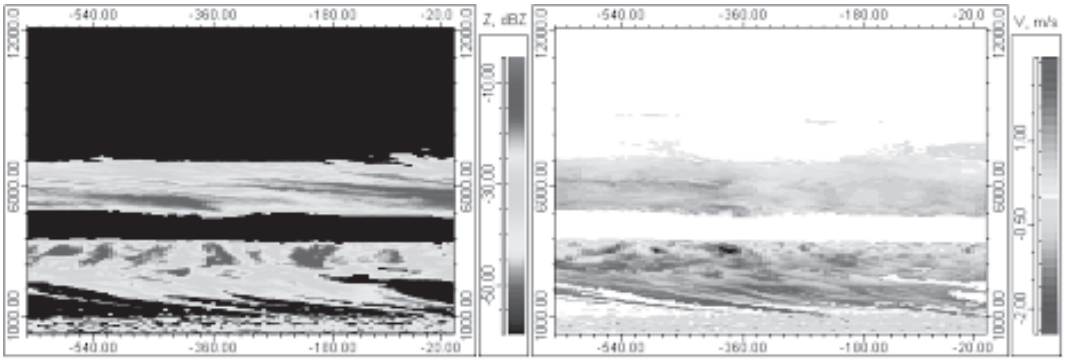


**Fig. 9.** *Middle and low layer clouds*

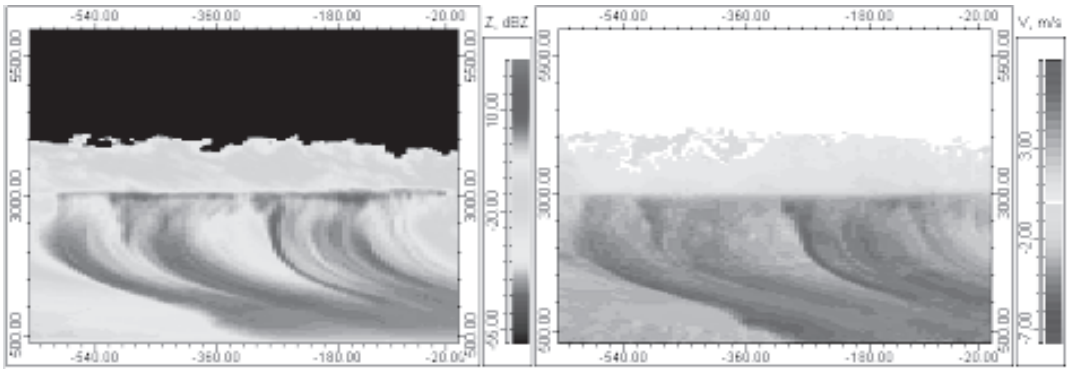


**Fig. 10.** *Precipitating clouds*

reach the ground in this case. The latter takes place in Fig. 10, where a heavy rain situation is illustrated.

Reflections from the atmospheric boundary layer can be seen in Fig. 8 and 9. Such reflections exist under the conditions of the clear air atmosphere and arrive from the heights up to about 2 km. A great deal of experimental data has already been accumulated and some general properties of the reflections have been determined [22-24]. For example, it has been found that: (i) the reflections are from closely spaced scatterers, (ii) the maximum scattering activity occurs in the noon and the minimum is at night, and (iii) in

summer the activity reaches its maximum. Various hypotheses have been put forward in order to explain the nature of the discussed reflections. Air turbulence, air layers, aerosols, insects, and birds have been considered as possible scatterers. However, any of these hypotheses can explain simultaneously all principal features of the boundary layer reflections.

## 4. 95 GHz Cloud Radar

The first version of the 95 GHz Doppler cloud radar was completed and tested in our Institute in 1999. In 2001, this radar was upgraded to perform polarimetric measurements. A photo of the radar system is given in Fig. 11. The measured parameters and technical characteristics of the radar are given in Tables 1 and 2, respectively. A simplified block diagram of the radio frequency part of the radar is shown in Fig. 12.

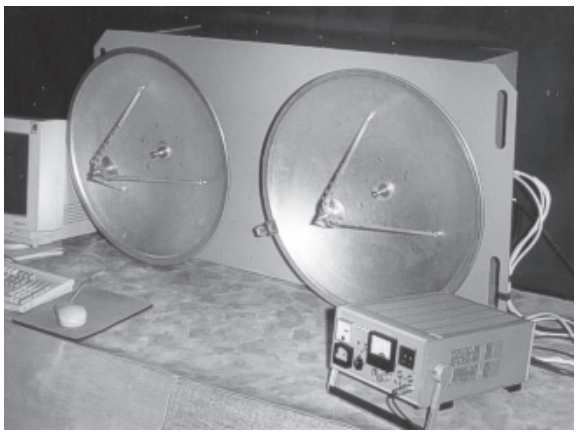

**Fig. 11.** *A photo of the 95 GHz radar system*

The separate 0.5-meter parabolic antennas are used for the transmitter and receiver ends. A polarization independent illuminator is used in the both antennas. In order to realize polarimetric measurements, ferrite quasioptical polarization manipulators are introduced between the receiver and its antenna, as well as between the transmitter and corresponding antenna. The manipulators are computer controlled allowing to obtain the pulse-to-pulse variation of the polarization of transmitted pulses and measurement of co- and cross-polarized components of the backscattered signals.

The transmitter is based on a 4 kW spatial-harmonic magnetron with cold secondary-emission cathode and a hard-tube modulator. The pulse duration is software controlled between 0.05 μs and 0.4 μs, and the maximum pulse repetition frequency is 5 kHz.

The radar receiver was built by using a scheme with the double frequency conversion. The first local oscillator is realized on a chain which consists of a highly stable, tunable oscillator operating at a frequency of about 10 GHz, a frequency multiplier, and a 95 GHz amplifier. The second local oscillator is a voltage-controlled generator with a maximum frequency deviation of 50 MHz. It is included in the loop for automatic frequency control.

The signal channel after the second mixer includes the stages of time-varying and manual gain control which provide the total dynamic range of 90 dB. Following these stages, the received signals are fed to a quadrature demodulator together with the output of a coherent oscillator (COHO). The outputs of the demodulator are used for phase and amplitude measurements in the data acquisition system.

## 5. Side-Looking Airborne Radar

### *5.1. Radar Characteristics*

The radar system consists of the 95 and 36 GHz channels with the corresponding antennas, transmitters, receivers, and signal pre-processing units as shown in Fig 13. A single interface unit and a host computer are used for both channels. The radar system also contains a navigation and orientation system (NOS), which include the GPS receiver, the autonomous gyroscope angle sensors, and an altimeter. The NOS is introduced in order to account for the variations of aircraft altitude, pitch angle, roll, and bank, necessary to produce a high quality radar image of the sea surface. The general characteristics of the radar system are given in Table 3.

A single antenna is used in the 8 mm wave channel for both the transmitter and receiver. The

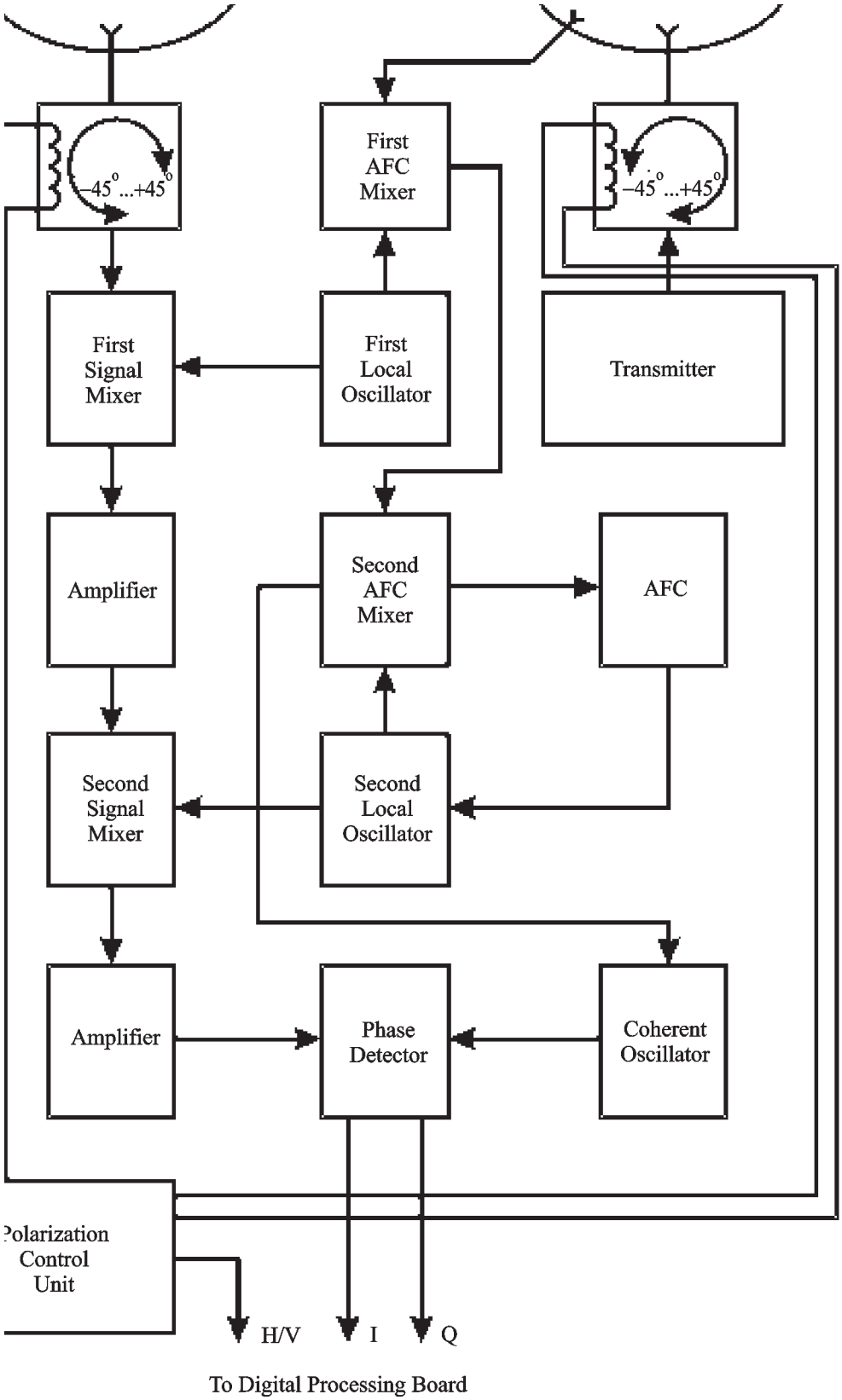


**Fig. 12.** *A simplified block diagram of the radio frequency part of the 95 GHz radar*

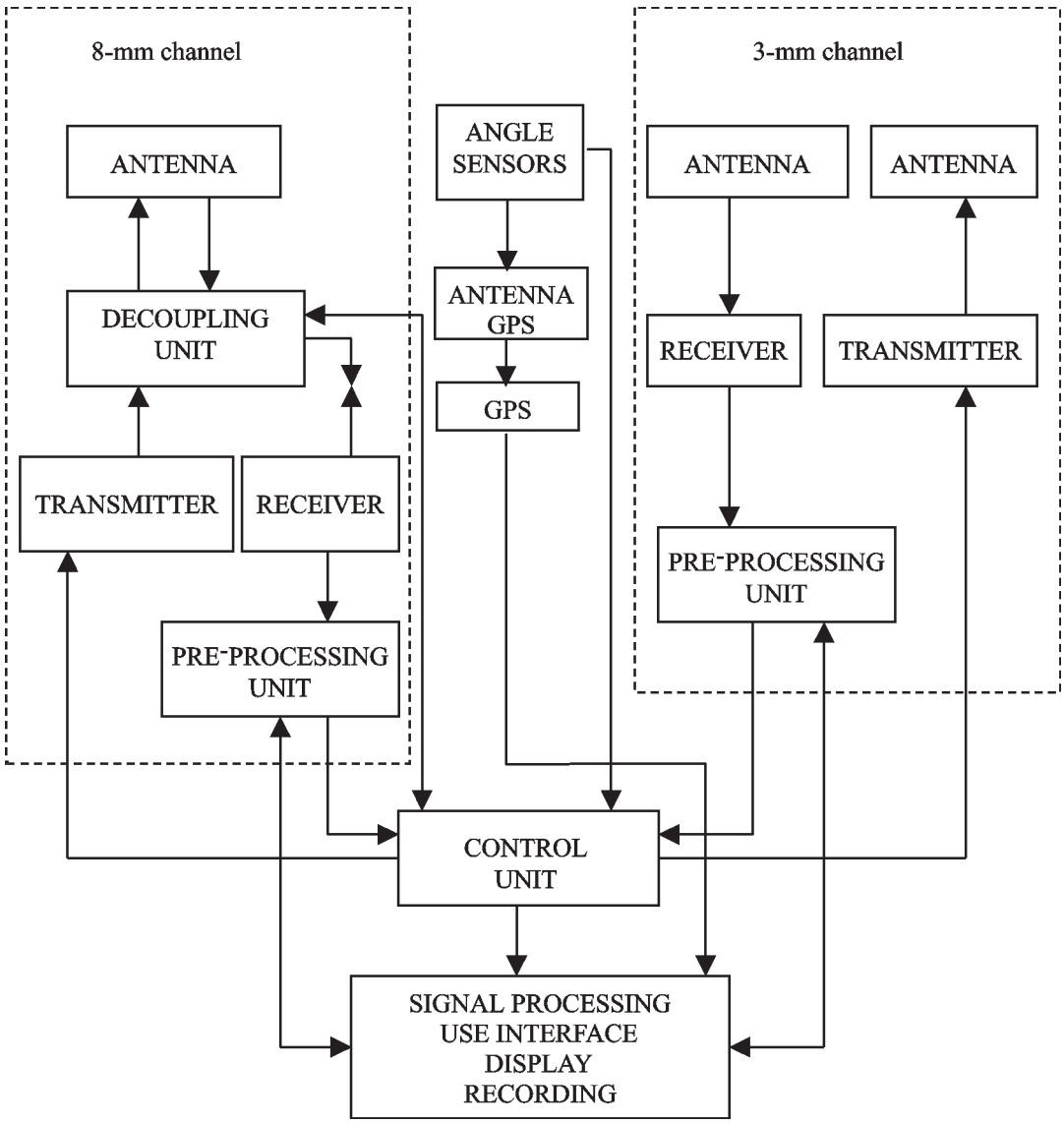


**Fig. 13.** *Block diagram of the dual frequency radar system*

receiver and transmitter are decoupled by means of a circulator and a pin-modulator. An original "dielectric waveguide – diffraction grating" antenna with V-V polarisation is used [25]. It has a planar construction with the dimensions of $100\times30\times5$ cm$^3$. The antenna forms a beavertail radiation pattern of $0.5°\times40°$, with the gain of 37 dB, and a side lobe level of $-20$ dB.

The problem of the transmitter-receiver decoupling in the 3 mm-wave channel is solved by the application of two separate identical antennas for the receiver and the transmitter ends. The antennas are of horn-parabolic type, where a parabolic cylinder is used as the reflection surface. Metal sheets overlap the end surfaces of the cylinder in order to reduce the side-lobes which are –18 dB down. A plane sub-reflector is introduced in order to decrease the antenna dimensions. The radiation pattern of these antennas is similar to that of the 8 mm-wave antenna.

The receivers for both radar channels have been built by using a scheme with the double frequency conversion and with a frequency control loop. Special efforts have been made to obtain a large

**Table 3.** *General characteristics of the dual frequency radar system*

| | | |
|---|---|---|
| Transmitted frequencies, GHz | 36.8±0.5 | 95±0.5 |
| Peak transmit power, kW | 20 | 4 |
| Pulse length, μs | 0.05 – 0.4 | 0.05 – 0.4 |
| Pulse repetition frequency, kHz | 5 | 5 |
| Receiver noise figure, dB | 4.5 | 8 |
| Dynamic range, dB | 60 | 60 |
| Tilt angles, degree | from 30 to 70 | from 30 to 70 |
| Beam width in azimuthal plane, degree | 0.5 | 0.5 |
| Polarization | Vertical | Vertical |
| Resolution in the flight perpendicular direction | Better than 30 m | Better than 30 m |
| Resolution in azimuthal direction (from the flight altitude of 4 km) | Better than 60 m | Better than 60 m |
| Width of the instantaneous observation area (from the flight altitude of 4 km), km | 8.5 | 8.5 |
| DC supply voltage, V | 28 | |
| Watt consumption (max) | 1500 | |
| Total weight, kg | 70 | |

dynamic range of the receiver, low level of the phase noise, and to simultaneously satisfy linearity of the control characteristics.

During the first experiments, the radar system was installed on a helicopter MI-8. Due to small dimensions of the radar, it was possible to place the radar just in an open door of the helicopter, as is shown in Fig. 14.


**Fig. 14.** *The dual frequency radar system installed on a helicopter*

### *5.2. Oil-Spill Detection*

The detection of oil spills by means of the side-looking radars or SAR systems usually lies in the analysis of reflectivity charts [12, 13, 26]. The presence of an oil film on the water surface leads to smoothing the surface, causing a reduction of the backscattering reflectivity coefficient which is readily detected by corresponding analysis of the radar returns. So far, the capabilities to detect oil spills with side-looking radars or SAR systems have mainly been demonstrated in the experiments undertaken over the sea or ocean surfaces. The first measurement campaign with the above described radar system dealt with the investigation of oil films on the river and lake surfaces. This campaign was organized in September 1997 near Nizshniy Novgorod, Russia, in cooperation with the Institute of Radio Physics and Electronics of the Ukrainian Academy of Sciences and the Research and Development Institute of Radio Technical Measurements.

Two main peculiarities of the oil-spill detection on the river and lake surfaces should be

mentioned. Firstly, the signal of a relatively small intensity reflected from the water surface is usually present in the receiver output together with the rather intense signals reflected from the river or lake banks. Therefore the receivers with a large dynamical range and a rather fast time varying gain control are necessary. The transient processes in the receivers should also be minimized to a great extent. Secondly, the radar contrast of oil spills on such surfaces is typically small compared with that on the sea or ocean surfaces because of the relatively small amplitudes of the surface waves on slick-free surfaces. Nevertheless, the experiments have shown that the radar system developed has a large potential for oil-spill detection even in case of rather small wind. For example, the radar contrast of an oil slick shown in Fig. 15 and 16 is about 6 dB. This slick was detected when the maximum amplitude of the surface waves on the slick-free surface was only 1 cm. The thickness of the oil film was about 0.05 mm.

Another series of experiments have been organized dealing with the detection of oil spills in a spool of 20×10 m, which is shown in Fig. 17. An oil film has covered the half of the pool. This part of the spool on the radar image is markedly different from the slick-free part of the pool, as is shown in Fig. 18. There was practically no wind during the measurements, and the amplitude of the surface waves was smaller

**Fig. 15.** *Optical image of an oil slick on a river*

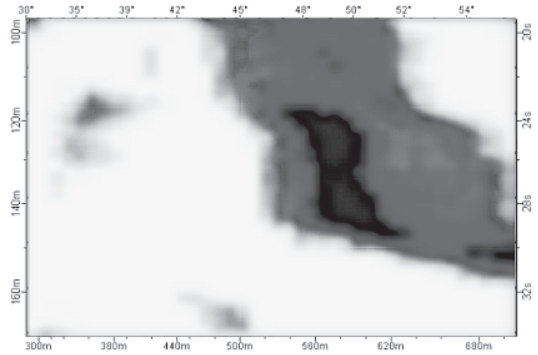


**Fig. 16.** *Radar image of the oil slick shown in Fig. 18*

**Fig. 17.** *Experimental pool, which is covered by half by oil film*

**Fig. 18.** *Radar image of the pool. The oil spill is shown by blue*

than 1 cm. It should be noted that the oil spill is detected even when the dimensions of the pool are relatively small as compared to the spatial resolution of the radar system.

Thus, the experiments have demonstrated a high capability of the developed radar system for the detection of oil spills on the river and lake surfaces. The results also indicate that the radar system can be effectively used for revealing and investigation of leakage from oil pipelines by means of detection of oil films on nearby rivers and lakes.

## 6. Conclusion

The development of radar systems for environmental studies has been initiated during the last years in the Institute of Radio Astronomy to meet the current demand for a new generation of such systems. The 95 and 36 GHz cloud radar systems and the dual-frequency 95 and 36 GHz side-looking airborne radar system have been developed, produced, and tested. These systems have embodied recent advances in the development of high power compact magnetron transmitters, mm-wave receivers, novel types of antennas, high speed digital signal processing boards, and signal processing technique. The obtained measurement results have demonstrated a high potential of the developed systems for various remote sensing applications.

## Acknowledgements

The authors would like to thank all of their colleagues at the Department of Microwave Electronics of the Institute of Radio Astronomy for their effort in the development of the cloud radars. The helpful cooperation with Dr. V. I. Kazantsev, Prof. B. A. Rozanov, Dr. A. C. Kurekin, and A. S. Gavrilenko is appreciated. The authors are indebted to Prof. L. Lytvynenko, Prof. K. Schünemann, and Dr. G. Peters for fruitful discussions and support.

## References

1. F. Pasqualucci, B. W. Bartram, R. A. Kropfli, and W. R. Moninger. J. Climate Appl. Meteor. 1983, **22**, pp. 758-765.
2. T. Takeda and M. Horiguchi. J. Atmos. Oceanic Technol. 1986, **64**, pp. 109-122.
3. R. M. Lhermitte. J. Atmos. Oceanic Technol. 1987, **4**, pp. 36-48.
4. J. B. Mead, A. L. Pazmany, S. M. Sekelsky, R. E. McIntosh. Proc. IEEE. 1994, **82**, pp. 1891-1906.
5. R. A. Kropfly and R. D. Kelly. Meteor. Atmos. Phys. 1996, **59**, pp. 105-121.
6. O. Danne, M. Quante, E. Raschke, and C. Weitkamp. Phys. Chem. Earth (B). 1999, **24**, pp. 167-171.
7. K. P. Moran, B. E. Martner, M. J. Post, R. A. Kropfli, D. C. Welsh, and K. B. Widener. Bull. Amer. Meteor. Soc. 1998, **79**, pp. 443-455.
8. V. Bormotov, G. Peters, K. Schünemann, D. Vavriv, V. Vinogradov, and V. Volkov. Proc. of the Millennium Conf. on Antennas and Propagation. Davos, Switzerland, 2000, p. 319.
9. V. Bormotov, G. Peters, K. Schünemann, D. Vavriv, V. Vinogradov, and V. Volkov. MST9 – COST 76 Workshop. France, Toulouse. 2000.
10. D. M. Vavriv. "Physics and Engineering of Millimeter and Sub-Millimeter Waves". Kharkov, Ukraine, 2001, pp. 85-89.
11. M. Jenett, V. Kazantsev, A. Kurekin, K. Schünemann, D. Vavriv, V. Vinogradov, and V. Volkov. Int. Geoscience and Remote Sensing Symposium. Hamburg. 1999.
12. N. Bartsch, K. Gruner, W. Keydel, and F. Witte. IEEE Trans. Geosci. Remote Sensing. 1987, **GE-25**, pp. 677-690.
13. E. N. Belov, et al. Proc. of 7-th Int. Crimean Microwave Conf. Sept. 1997, Sevastopol, Ukraine, pp. 56-61.
14. K. Schünemann, A. Timchenko, and A. Serebryannikov. "A new model of electromagnetic wave scattering from sea surface with and without oil films" (in press).
15. I. M. Vigdorchik, V. D. Naumenko, V. P. Timofeev. Doklady Ukr. Akademii Nauk. 1975, **A**, No. 7, pp. 634-637 (in Russian).
16. V. D. Naumenko, K. Schünemann, and D. M. Vavriv. Electronics Letters. 1999, **35**, pp. 1960-1961.
17. K. Schünemann, S. Sosnitskiy, and D. M. Vavriv. IEEE Trans. on ED. 2001, **48**, pp. 993-998.
18. V. D. Naumenko, K. Schünemann, V. Ye. Semenuta, D. M. Vavriv, and V. A. Volkov. Proc. of the 22-nd Int. Conf. on Infrared and Millimeter Waves. USA, 1997, pp. 42-43.
19. K. Schünemann, B. Trush, D. Vavriv, and V. Volkov. Proc. of the 30-th European Micr. Conf. Paris, 2000.
20. M. Jenett, R. Kozshin, K. Schünemann, D Vavriv, and V. Vinogradov. Proc. of the Int. Geoscience and Remote Sensing Symposium. Hamburg, 1999.

21. D. M. Vavriv, V. V. Vinogradov, and S. A. Razbejko. Radio Physics and Radio Astronomy. 2001, **6**, No. 3, pp. 212-221.
22. D. Atlas. Advances in Radar Meteorology. Academic Press. 1964.
23. H. Ottersten. Radio Science. 1969, **4**, No. 12, pp. 1251-1255.
24. R. M. Lhermitte. Journal of the Atmospheric Sciences. 1966, **23**, pp. 575-591.
25. A. P. Yevdokimov, and V. V. Krizhanovsky. Radioelectronics. 1996, **39**, pp. 54-61.
26. J. T. Macklin. GEC J. of Research. 1992, **10**, pp. 19-27.

## Радиолокаторы миллиметрового диапазона длин волн для исследования параметров окружающей среды

**Д. М. Ваврив, В. А. Волков, В. Н. Бормотов, В. В. Виноградов, Р. В. Кожин, Б. В. Труш, А. А. Беликов, В. Е. Семенюта**

В статье обобщены результаты работ, инициированных в последнее время в Радиоастрономическом институте НАН Украины, по созданию радиолокаторов миллиметрового диапазона длин волн. Разработанные радиолокационные системы включают метеорологические локаторы и самолетный радиолокатор бокового обзора. Они дают возможность проведения измерений в 8- и 3-мм диапазонах длин волн с высоким пространственным разрешением в реальном времени. В статье обсуждаются вопросы построения этих инструментов, использованные новые технические решения и методы обработки сигналов. Представлены также результаты проведенных измерений.

## Радіолокатори міліметрового діапазону довжин хвиль для дослідження параметрів навколишнього середовища

**Д. М. Ваврів, В. А. Волков, В. М. Бормотов, В. В. Виноградов, Р. В. Кожин, Б. В. Труш, О. О. Бєліков, В. Є. Семенюта**

У статті узагальнені результати робіт, ініційованих останнім часом у Радіоастрономічному інституті НАН України, по створенню радіолокаторів міліметрового діапазону довжин хвиль. Розроблені радіолокаційні системи включають метеорологічні локатори і літаковий радіолокатор бічного огляду. Вони дають можливість проведення вимірювань у 8- і 3-мм діапазонах довжин хвиль з високим просторовим розділенням у реальному часі. У статті обговорюються питання побудови цих інструментів, використані нові технічні рішення і методи обробки сигналів. Представлено також результати проведених вимірювань.